Letters

A Load-Independent Wireless Power Transfer System With Multiple Constant Voltage Outputs

Chenwen Cheng, Weiguo Li, Zhe Zhou, Zhanfeng Deng, and Chris Mi, *Fellow, IEEE*

***Abstract*—A novel wireless power transfer (WPT) system is proposed to power the gate drivers in a multilevel converter to achieve a high insulation level. There are two requirements for the proposed WPT system. First, the WPT system should contain multiple outputs, each corresponding to one gate driver. Second, a constant voltage source is needed for each gate driver. For a multiload WPT system, it is challenging but necessary to realize independent power control of each load. To achieve this goal, the repeater unit consisting of two repeater coils is designed to power a load. Many loads can be powered simultaneously by using multiple repeater units together. The *LCC*-S compensation topology is adopted for the proposed WPT system. Constant voltage outputs are obtained for all the loads when neglecting the coil's parasitic resistance. An experimental platform with six loads was developed to validate the proposed WPT system.**

***Index Terms*—Constant voltage output, LCC-S, load-independent, multiple loads, wireless power transfer (WPT).**

I. Introduction

ISOLATED power supplies are required for the gate drivers in a multilevel converter because the reference potentials of the power switches are different. In [1] and [2], several high-frequency transformers were used with their primary winding connected in series. The secondary windings of these transformers provided multiple isolated outputs for the gate drivers. Another solution was provided in [3] that collected power from the storage capacitor and the isolated power supplies can be eliminated. However, this kind of solution may fail during a power outage.

The wireless power transfer (WPT) technology [4] provides an ideal solution for powering the gate drivers in a multilevel converter because no direct contact is needed [5]. The air is a good insulation medium, which can provide high insulation level. Although most of the conventional WPT systems can only power one load [6], the WPT system with multiple outputs is drawing more and more attentions recently [7]–[10]. In [7], multiple receiving coils with different resonant frequencies are designed. The receiving coil that has the same resonant frequency with the transmitter's frequency will receive power while the others will not. However, all the receiving coils cannot obtain power simultaneously. A different WPT system with multiple outputs was designed in [8] for the LED lighting system. The multiple LEDs are connected in parallel across the same receiving coil via the *CLC* circuits. However, the outputs in this system are not isolated, which is not suitable for the proposed application. The multiload WPT systems using the repeater units were proposed in [9]–[11] where constant load currents were obtained by using different compensation methods. However, the constant current source is not suitable for driving the gate driver where a constant voltage source is preferred. Thus, a conversion unit is needed to transform these constant current outputs into constant voltage outputs before they are used to power the gate drivers, which increases the system complexity.

A novel WPT system with multiple outputs is proposed in this letter. The coil structure based on the repeater unit in [9] is adopted in this letter. For each transmitting coil, the LCC compensation is used. For each receiving coil, a compensation capacitor is connected in series with the coil. Constant voltage outputs can be obtained for all the loads, which facilitate the independent load power control. An experimental setup with six loads was developed to validate the proposed WPT system.

II. System Modeling

A. System Description

Fig. 1 shows the structure of the proposed WPT system with N loads. There are $(N+1)$ units in the WPT system, which are transmitting unit #0, repeater units #n ($n = 1, 2, \ldots, N-1$), and receiving unit #N. In transmitting unit #0, a high-frequency ac power source $\boldsymbol{V}_0$ with the angular frequency ω_0 is used to excite transmitting coil L_{0_t}. In repeater unit n, there are two repeater coils, namely L_{n_r} and L_{n_t}, which receives power from its previous unit and transmits power to the next unit, respectively. The subscript "r" and "t" represent "receiving" and "transmitting," respectively. For receiving unit #N, only receiving coil

Manuscript received July 15, 2019; revised August 15, 2019; accepted August 31, 2019. Date of publication September 8, 2019; date of current version January 10, 2020. This work was supported by the Global Energy Interconnection Research Institute Co., Ltd., (GEIRI) under Grant GEIRI-DL-71-17-011 (State Grid Sci. & Tech. Project: Research on the Magnetic-Resonant Wireless Power Transfer Technology for the High-Voltage Converter Valve in FACTS). *(Corresponding author: Chris Mi.)*

C. Cheng and C. Mi are with the San Diego State University, San Diego, CA 92182 USA (e-mail: cheng.cwen@gmail.com; mi@ieee.org).

W. Li, Z. Zhou, and Z. Deng are with the State Key Laboratory of Advanced Power Transmission Technology (Global Energy Interconnection Research Institute), Changping, Beijing 102211, China (e-mail: lwgmb90549@sina.com; zhouzhe@geiri.sgcc.com.cn; iphone21@sina.com).

Color versions of one or more of the figures in this article are available online at http://ieeexplore.ieee.org.

Digital Object Identifier 10.1109/TPEL.2019.2940091

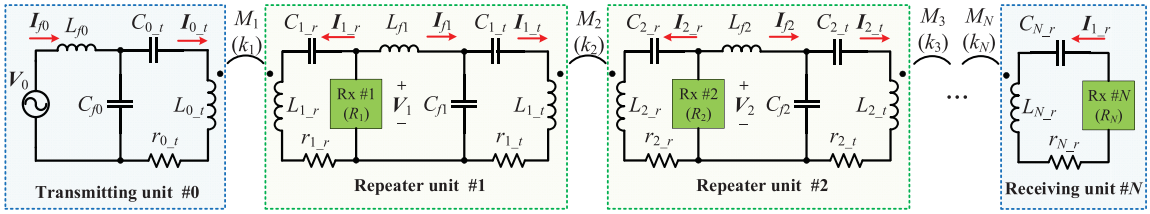

Fig. 1. Structure of the proposed WPT system.

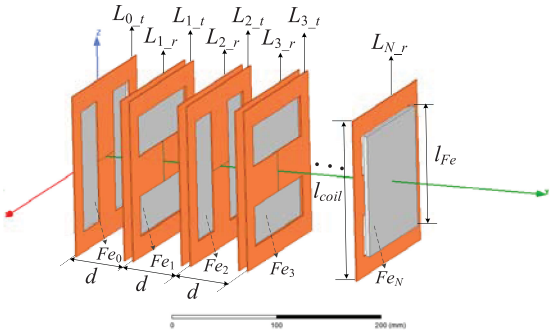

Fig. 2. Coil structure used in the proposed WPT system.

L_{N_r} exists. r_{n_r} and r_{n_t} are the parasitic resistances of L_{n_r} and L_{n_t}, respectively. In unit #*n*, an *LCC* circuit consisting of L_{fn}, C_{fn}, and C_{n_t} is used to compensate transmitting coil L_{n_t}, while a compensation capacitor C_{n_r} is connected in series with receiving coil L_{n_r}, which form an *LCC*-S topology for each transmitter-receiver pair. The receiving circuit Rx #*n* is connected across receiving coil L_{n_r} in the unit #*n* ($n = 1, 2, \ldots, N$) as shown in Fig. 1, which contains an uncontrolled rectifier and a dc–dc converter to transform the received ac power to a stable dc output for the gate drivers. In this case, the output dc voltage of Rx #*n* is 15 V. Considering that the voltage across the rectifier and the current flowing through the rectifier are in phase, the total receiving circuit Rx #*n* is resistive [4] and will be modeled as a load resistor R_n in the following analysis. $\boldsymbol{I}_{fn}$, $\boldsymbol{I}_{n\_t}$, and $\boldsymbol{I}_{n\_r}$ are the currents flowing through L_{fn}, L_{n_t}, and L_{n_r}, respectively, the positive directions of which are defined in Fig. 1. The power is transferred between two adjacent units #$(n-1)$ and #*n* via the magnetic coupling between L_{n-1_t} and L_{n_r}. The mutual inductance and the coupling coefficient between L_{n-1_t} and L_{n_r} are defined as M_n and k_n, respectively. The other couplings should be as small as possible, which can be realized by the coil structure discussed in the following section.

B. Coil Design

In order to achieve the magnetic decoupling between nonadjacent coils and the two coils in same repeater unit, the coil structure proposed in [9] and [10] is used in this letter as shown in Fig. 2, which is briefly described below. The bipolar coils are adopted and the two coils in the same repeater unit are placed perpendicularly, so that the magnetic coupling between them can be eliminated because their magnetic fields are orthogonal

TABLE I
SIMULATED COUPLING COEFFICIENTS

k_{1r_1t}	k_{1r_2r}	k_{1r_2t}	k_{1_2}
0.0001	0.0001	0.0064	0.257

[10]. Moreover, the ferrite plate F_{en} $(n = 1, 2, \ldots, N)$ is inserted in each unit. As a result, the magnetic coupling between nonadjacent coils can be suppressed further due to the magnetic insulation effect of the ferrite plates.

In Fig. 2, the distance between any two adjacent units is $d = 60$ mm; both the coils and the ferrite plates are square and their side length are $l_{\text{coil}} = 160$ mm and $l_{Fe} = 120$ mm, respectively. Due to the symmetric characteristic of the coil structure, only unit #1 and #2 are simulated using MAXWELL. k_{1r_1t}, k_{1r_2r}, k_{1r_2t}, and k_2 are defined as the coupling coefficients between L_{1r} and L_{1t}, L_{1r} and L_{2r}, L_{1r} and L_{2t}, L_{1t} and L_{2r}, respectively, which are listed in Table I. It can be seen that compared to k_2, the other couplings are very small and can be neglected.

C. System Analysis

The following resonant condition should be met:

$$\omega_0^2 = \frac{1}{L_{n\_r}C_{n\_r}} = \frac{1}{L_{fn}C_{fn}} = \frac{1}{L_{n\_t}C_{n\_t}} + \frac{1}{L_{n\_t}C_{fn}}. \quad (1)$$

The quality factor of L_i is defined as

$$Q_i = \omega_0 L_i / r_i \quad (2)$$

where "*i*" indicates the coil number. According to Section II-B, the inductances and quality factors of all the coils, the mutual inductances and the coupling coefficients between L_{n-1_t} and L_{n_r} are identical, i.e.,

$$\begin{cases} L_{0\_t} = L_{1\_r} = L_{1\_t} = L_{2\_r} = \cdots = L_{N\_r} = L \\ Q_{0\_t} = Q_{1\_r} = Q_{1\_t} = Q_{2\_r} = \cdots = Q_{N\_r} = Q \\ M_1 = M_2 = \cdots = M_N = M, k_1 = k_2 = \cdots = k_N = k. \end{cases} \quad (3)$$

The reflection impedances in L_{n_t} and L_{n_r} are used to help analyze the system, which can be defined as

$$\begin{cases} Z_{n\_t} = \dfrac{(\omega_0 M_{n+1})^2}{r_{n+1\_r} + Z_{n+1\_r}}, & n = 0, 1, \ldots, N-1 \\ Z_{n\_r} = \dfrac{R_n(\omega_0 L_{fn})^2}{R_n(r_{n\_t} + Z_{n\_t}) + (\omega_0 L_{fn})^2}, & n = 1, 2, \ldots, N-1. \end{cases} \quad (4)$$

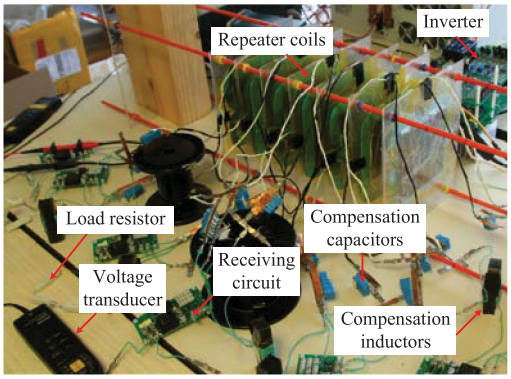

Fig. 3. Experimental platform with six loads.

For L_{N_r}, the reflection impedance is $Z_{N\_r} = R_n$. Based on (4), the reflection impedance in each coil can be calculated iteratively from the last coil to the first one. Then, $\boldsymbol{I}_{n\_r}$, $\boldsymbol{V}_n$, and $\boldsymbol{I}_{n\_t}$ in each unit can be calculated as

$$\begin{cases} \boldsymbol{I}_{n\_r} = -j\omega_0 M_n \boldsymbol{I}_{n-1\_t} / \\ \qquad (r_{n\_r} + Z_{n\_r}) \\ \boldsymbol{V}_n = j\omega_0 M_n \boldsymbol{I}_{n-1\_t} + \boldsymbol{I}_{n\_r} \cdot r_{n\_r}, \\ \boldsymbol{I}_{n\_t} = \boldsymbol{V}_n / (j\omega_0 L_{fn}), \end{cases} \begin{array}{l} n = 1, 2, \ldots N \\ n = 1, 2, \ldots, N \\ n = 0, 1, 2, \ldots, N-1. \end{array} \tag{5}$$

The load voltage V_n can be calculated iteratively using (5). In an ideal condition, the coil's parasitic resistance is very small and can be neglected. With this assumption, V_n can be simplified by setting $r_{n\_r} = r_{n\_t} = 0$ in (4) and (5) as

$$\boldsymbol{V}_n = \boldsymbol{V}_{n-1} \cdot M_n / L_{f(n-1)}, \quad n = 1, 2, 3, \ldots, N. \tag{6}$$

It can be seen from (6) that equal load voltage can be obtained, i.e., $\boldsymbol{V}_1 = \boldsymbol{V}_2 = \boldsymbol{V}_3 = \cdots = \boldsymbol{V}_N$, when the following equations are met:

$$L_{f0} = M_1, L_{f1} = M_2, \ldots, L_{f(N-1)} = M_N. \tag{7}$$

After the mutual inductances are measured, the compensation inductance L_{fn} can be obtained based on (7). Together with the coil's self-inductance, the compensation capacitance C_{n_r}, C_{n_t}, and C_{fn} can be calculated based on (1).

Considering (3), (7) can be simplified as

$$L_{f0} = L_{f1} = L_{f2} = \cdots = L_{f(N-1)} = M. \tag{8}$$

It should be pointed out that the proposed WPT system cannot only be used in the application where the mutual inductances are identical, but also in the application with different mutual inductances. As long as (7) is met, equal load voltages can be obtained. The condition in (8) is only a special case in the gate driver application in this letter.

III. Experimental Results

A. Experimental System Setup

An experimental platform with six loads has been developed as shown in Fig. 3. An H-bridge inverter is used to generate a 200 kHz ac power source. The Litz wire is adopted to fabricate the repeater coils to decrease the influence of the skin effect.

TABLE II
System Parameters

Parameter	*Value*	*Parameter*	*Value*	*Parameter*	*Value*
V_{dc}	25 V	f_s	200 kHz	L_{0_r}~L_{6_r}	93 μH
L_{f0}~L_{f5}	22.3 μH	C_{f0}~C_{f5}	28.4 nF	C_{1_r}~C_{6_r}	6.81 nF
C_{0_r}~C_{5_t}	8.96 nF	k	0.24	Q	280
Maximum AC/AC efficiency	91.3%	*DC/DC efficiency*	63.7%		

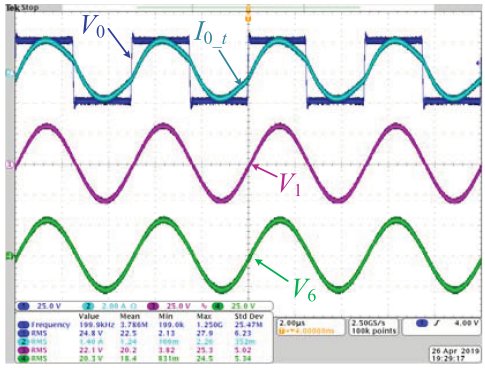

Fig. 4. Experimental waveforms with load resistors.

The dimensions of the coils and ferrite plates are consistent with the MAXWELL simulation model in Section II-B. The parameter calculation method is given as follows.

1) After the system is fabricated, the coil inductance L_{n_r}, L_{n_t} and mutual inductance M_n can be measured using the *LCR* meter or impedance analyzer.
2) $L_{f(n-1)}$ can be set equal to M_n based on (7).
3) The values of the compensation capacitances C_{n_r}, C_{n_t} and C_{fn} can be calculated using (1).

Table II lists the detailed parameters of the system.

B. Experimental Results

First, power resistors instead of the receiving circuits are used as the loads. Fig. 4 shows the experimental waveform with load resistors acquired by the oscilloscope when the normalized load power is 0.3. Only V_0, I_{0_t}, V_1, and V_6 are given due to the limited channels of the oscilloscope. As can be seen, the load voltages are in phase, and the amplitudes of them are nearly the same.

Fig. 5 shows the variation of the load voltages against the increasing load power where the solid lines represent the calculated load voltages using (5) considering the parasitic resistance of the coil, and the dot points represent the measured load voltages. All the load resistances are identical to facilitate the comparison, i.e.,

$$R_1 = R_2 = \cdots = R_N = R_L. \tag{9}$$

All load voltages and load power are normalized by dividing their base values defined as

$$V_b = V_0, \quad R_b = \omega_0 M, \quad P_b = V_b^2 / R_b. \tag{10}$$

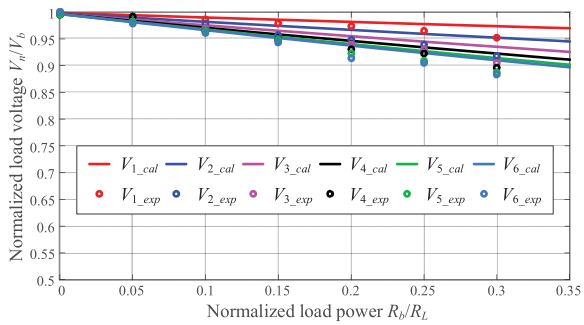

Fig. 5. Load voltage variations against the increasing load power.

TABLE III
MEASURED SYSTEM EFFICIENCY

Normalized load power	0.05	0.1	0.15	0.2	0.25	0.3
Total load power/W	5.53	9.95	14.31	19.30	23.93	27.60
Efficiency	82.1%	88.1%	89.9%	90.6%	91.3%	89.3%

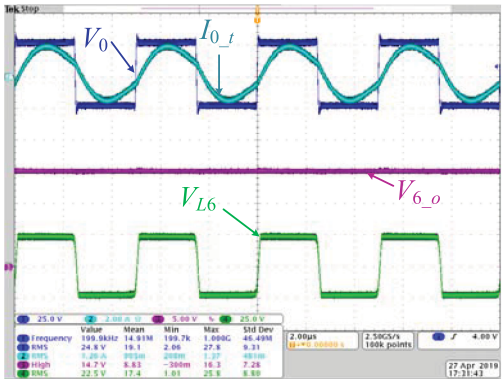

Fig. 6. Experimental waveforms of the receiving circuit Rx #6.

Assuming that the load voltage drop is small and all load voltages are nearly equal to V_0, the normalized load power can be calculated as

$$P_{Ln\_\mathrm{norm}} = P_{Ln}/P_b \approx R_b/R_L. \tag{11}$$

Thus, the normalized load power can be represented by R_b/R_L. It can be seen from Fig. 5 that the load voltages decrease gradually as the load power increases. That is because the coil's parasitic resistance consumes some power. In Fig. 5, the load voltage drop is small and acceptable.

Table III lists the system efficiency with different power levels, which is defined as the sum of all the load powers divided by the total output power of the inverter. The maximum efficiency can reach 91.3%, which is very high considering that there are totally six loads in the system.

Then, the receiving circuit consisting of a rectifier and a dc/dc converter is applied in the experimental system. The waveforms of one of the receiving circuits, Rx #6, is shown in Fig. 6. V_{L6} is the voltage across the rectifier, which is a square waveform due to the different conduction states of the rectifier. V_{6_o} is the output of the dc/dc converter, which is a stable dc voltage source of 14.7 V. The output power of each receiving circuit in Fig. 6 is 3 W and the dc-to-dc efficiency is 63.7%.

IV. CONCLUSION

A novel WPT system is proposed in this letter, which can be used to power the multiple gate drivers in a multilevel converter. The repeater unit is used in the design process, which can achieve magnetic decoupling between any nonadjacent coils and the two coils in the same repeater unit. The *LCC*-S compensation topology is adopted, and the constant load voltages can be obtained. An experimental platform with six loads is developed to validate proposed WPT. The maximum system efficiency can reach 91.3%.

REFERENCES

[1] A. Sepehr, M. Saradarzadeh, and S. Farhangi, "High-voltage isolated multioutput power supply for multilevel converters," *Turkish J. Elect. Eng. Comput. Sci.*, vol. 25, no. 4, pp. 3319–3333, Jan. 2017.

[2] J. Afsharian, B. Wu, and N. Zargari, "High-voltage isoltated multiple outputs DC/DC power supply for GCT gate drivers in medium voltage (MV) applications," in *Proc. 28th Annu. IEEE Appl. Power Electron. Conf. Expo.*, 2013, pp. 1480–1484.

[3] D. M. Raonic, "SCR self-supplied gate driver for medium-voltage application with capacitor as storage element," *IEEE Trans. Ind. Appl.*, vol. 36, no. 1, pp. 212–216, Jan./Feb. 2000.

[4] S. Li and C. C. Mi, "Wireless power transfer for electric vehicle applications," *IEEE J. Emerg. Sel. Topics. Power Electron.*, vol. 3, no. 1, pp. 4–17, Mar. 2015.

[5] M. Takasaki, Y. Miura, and T. Ise, "Wireless power transfer system for gate power supplies of modular multilevel converters," in *Proc. IEEE 8th Int. Power Electron. Motion Control Conf.*, May 2016, pp. 3183–3190.

[6] Z. Zhang, H. Pang, A. Georgiadis, and C. Cecati, "Wireless power transfer—An overview," *IEEE Trans. Ind. Electron.*, vol. 66, no. 2, pp. 1044–1058, Feb. 2019.

[7] Y. Zhang, T. Lu, Z. Zhao, F. He, K. Chen, and L. Yuan, "Selective wireless power transfer to multiple loads using receivers of different resonant frequencies," *IEEE Trans. Power Electron.*, vol. 30, no. 11, pp. 6001–6005, Nov. 2015.

[8] Y. Li *et al.*, "Analysis, design and experimental verification of a mixed high order compensations-based WPT system with constant current outputs for driving multistring LEDs," *IEEE Trans. Power Electron.*, vol. 67, no. 1, pp. 203–213, Jan. 2020.

[9] C. Cheng *et al.*, "Load-independent wireless power transfer system for multiple loads over a long distance," *IEEE Trans. Power Electron.*, vol. 34, no. 9, pp. 9279–9288, Sep. 2019.

[10] C. Cheng, Z. Zhou, W. Li, C. Zhu, Z. Deng, and C. Mi, "A multi-load wireless power transfer system with series-parallel-series compensation," *IEEE Trans. Power Electron.*, vol. 34, no. 8, pp. 7126–7130, Aug. 2019.

[11] C. Cheng *et al.*, "A load-independent LCC-compensated wireless power transfer system for multiple loads with a compact coupler design," *IEEE Trans. Ind. Electron.*, to be published, doi: 10.1109/TIE.2019.2931260.